

Article title

An open source 16-channel fluidics system for automating sequential fluorescent *in situ* hybridization (FISH)-based imaging

Authors

Zhaojie Deng^a, Brian J. Beliveau^{a,b}

Affiliations

^aDepartment of Genome Science, University of Washington, Seattle, WA, United States

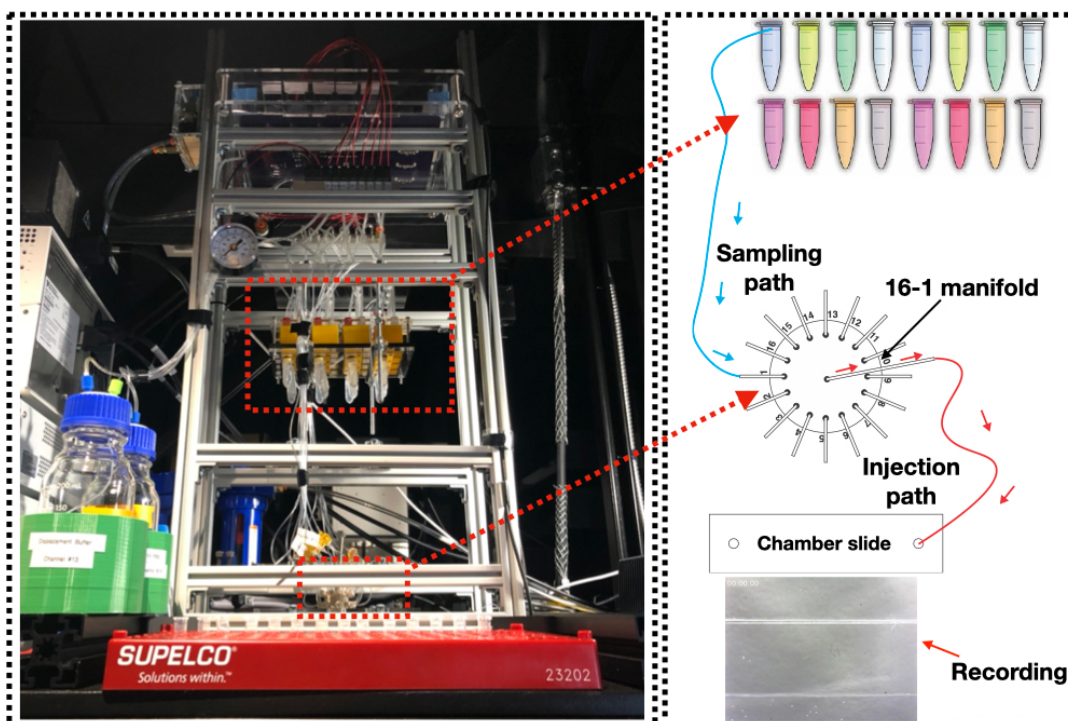
^bBrotman Baty Institute for Precision Medicine, Seattle, WA, United States

Corresponding author's email address and Twitter handle

beliveau@uw.edu, @oligopain

Abstract

Fluorescent *in situ* hybridization (FISH) can provide spatial information about DNA/RNA targets in fixed cells and tissues. However, the workflows of multiplexed FISH-based imaging that use sequential rounds of hybridization quickly become laborious as the number of rounds increases because of liquid handling demands. Here, we present an open-source and low-cost fluidics system that is purpose built for automating the workflows of sequential FISH-based imaging. Our system features a fluidics module with 16 addressable channels in which flow is positive pressure-driven and switched on/off by solenoid valves in order to transfer FISH reagents to the sample. Our system also includes a controller with a main printed circuit board that can control up to 120 solenoid valves and allows users to control the fluidics module via serial communication. We demonstrate the automatic and robust fluid exchange with this system by targeting the alpha satellite repeat in HeLa cell with 14 rounds of sequential hybridization and imaging. We anticipate that this simple and flexible system will be of utility to researchers performing multiplexed *in situ* assays in a range of experimental systems.



Keywords

Liquid handling, Sequential FISH-based imaging, Laboratory automation, Pneumatic driven, ESP32

Specifications table

Hardware name	Integrated Multichannel Fluidics System
Subject area	<ul style="list-style-type: none">• Engineering and materials science• Medical (e.g., pharmaceutical science)• Neuroscience• Biological sciences (e.g., microbiology and biochemistry)• Educational tools and open source alternatives to existing infrastructure
Hardware type	<ul style="list-style-type: none">• Imaging tools• Biological sample handling and preparation• Electrical engineering and computer science
Closest commercial analog	Microfluidics Unit – BRUKER. Available at: https://www.bruker.com/en/products-and-solutions/fluorescence-microscopy/super-resolution-microscopes/microfluidics-unit.html (Accessed: 28th January 2022). The fluidics system presented here has a controller that can control up to 120 channels and the built cost is at a fraction of that of the commercial system.
Open source license	GPL, MIT
Cost of hardware	USD5000
Source file repository	https://doi.org/10.17632/tkm4w7wp3v.1 ; https://github.com/dzhaojie/Fluidics-system-for-FISH

1. Hardware in context

Fluorescent *in situ* hybridization (FISH) is a technique that uses fluorescently labeled nucleic acid probes to target genomic and/or transcriptomic sequences of interest in cells and tissues through hybridization. After hybridization, the locations and abundances of the targets can be detected by fluorescence microscopy. Therefore, FISH enables researchers to obtain spatial genomic and transcriptomic information relevant to their research. Recent developments in FISH technology have focused on improving its multiplexing capability in order to efficiently detect more than a dozen genes and/or RNAs in one experiment by either spectral encoding [1], [2] or sequential hybridization [3], [4], [5], [6]. Recent advances in multiplexing strategies involve combining spectral encoding of the DNA/RNA targets with sequential hybridization of FISH readout probes to detect thousands of DNA/RNA species [7], [8], [9], [10]. Sequential FISH procedures usually involve many rounds of hybridization. During each round, readout probes are hybridized and imaged and their signal is removed by either one or two of these methods: photobleaching, toehold displacement of the readout probes, chemically stripping of the readout probes. Protocols for sequential FISH-based imaging are usually complicated and involve multiple liquid handling and/or exchange steps in each hybridization round. Therefore, they are time consuming and labor-intensive for manual implementation, preventing them from being widely adopted.

Commercially available liquid handling solutions [11], [12], [13] are either hard to adapt to sequential FISH-based imaging or are expensive when the rounds of imaging need to be scaled up. An open-source integrated automation solution capable of handling more than a dozen rounds of fluid exchange for sequential hybridization would help address this challenge. Integrated microfluidics platforms have been demonstrated to perform all assay steps in an entire FISH protocol [14]. However, these platforms can

only perform up to a dozen hybridization rounds and they are difficult to scale up. Other solutions utilize peristaltic pumps combined with rotative valves to automate fluid exchanges up to 24 rounds in imaging chambers [15] or with Lego-hardware to support up to 128 syringe pumps to input reagents into a peristaltic pump driven flow system [16]. While these solutions provide high-throughput automation, peristaltic pumps offer less stability in flow rate control for long-term experiment like sequential FISH more than a dozen rounds [17]. On the other hand, pressure-driven provides high stability and pulseless flow [17]. Here, we present an open source fluidics system with 16 channels individually driven by positive pressure for automation of sequential FISH-based imaging protocols. We show robust fluid exchange with the system through 14 rounds of fluorescent oligo hybridization (2 other channels were used for washing buffer and probe displacement buffer) to readout the primary probes at the alpha satellite in Hela cells. While maintaining a comparable dead volume (100 μ L) to commercial ones, this open source standalone fluidics system offers a custom designed sample loading module (no extra tool required) for conveniently loading probe solutions to significantly reduce experiment prep time. It can also be integrated with a microscope enabling users to run/test FISH-based imaging protocols easily in their own laboratories.

2. Hardware description

2.1 Design Overview

The fluidics system here was designed with full automation and minimized reagent cost in mind. It also was built with low cost and widely available components. It operates via positive pressure-driven flow to introduce FISH reagents to the sample. The positive pressure can come from any common laboratory compressed air source. The whole system includes a fluidics module and a PCB controller. An overview of the fluidics module is shown in Fig. 1. A compressed gas line runs first through a filter module (component R2) and then a pressure regulator (component R3). The pressurized gas is then distributed into 16 individual lines by a splitting manifold (component R6) and 2 solenoid valve and manifold assemblies (component SV1&SV2). These 16 gas lines (T4) can be individually addressed to pressurize a designated reservoir filled with FISH probes or washing buffer. The 16 fluid lines (T2) coming out of the reservoirs are then combined by a mini manifold (with 16 inlets and 1 inlet) and become a single fluid line connected directly to the inlet of a sample chamber. A sample loading module (not shown in the diagram) composed of an array of 16 custom designed and 3D-printed Eppendorf tube adapters (component E1 here) was designed and assembled for easy sample loading using conventional 2 mL Eppendorf tube (component b). A structural frame (not shown in the diagram) was built to organize all the components into a standalone machine.

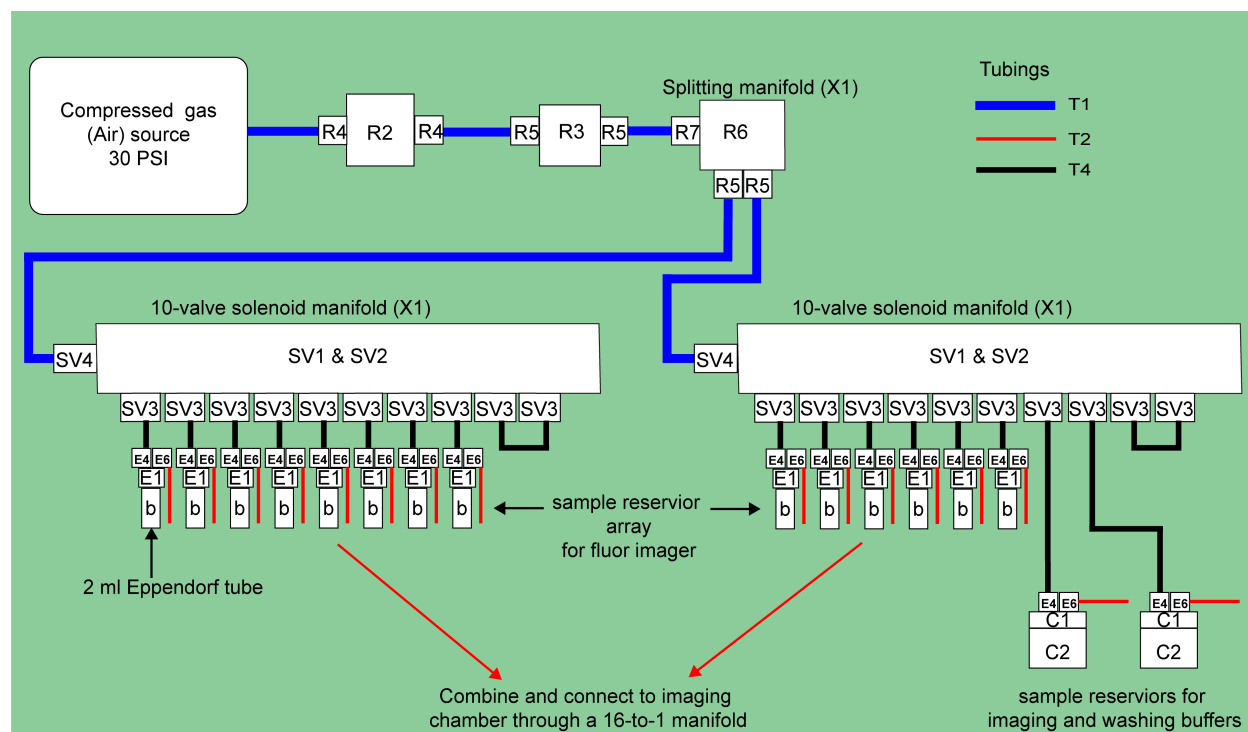


Fig. 1. Overall schematic of the fluidics module (pneumatic and fluidics components) designated by letters and numbers (as referenced to the Bill of materials)

2.2 Controller PCB

A controller was designed for controlling the on/off of the solenoid valves, the pressure regulator, and a flow rate sensor, as well as handling serial communication with the microscope PC running the imaging routines. The main PCB of the controller is based on the design in the open-source microfluidics control system by Craig Watson [18]. It uses Espressif ESP32 devkit C as microcontroller and PCA9698 as I/O expander. Here, the PCB can address up to 120 solenoid valves after adding 2 more PCA9698 chips. Additionally, an interface is also added for a flow rate sensor (MFS, ElveFlow) powered by 9 V and it uses analog pins to read in the voltage output by the sensor. The 9 V is provided by a 12 V to 9 V regulator. The interface for the pressure regulator is designed to control a commercial digital pressure regulator from (MPV, Proportion-Air). This controller handles all the messages from the PC through USB serial communication to operate the fluidics system.

2.3 User Interface

A user interface for flow rate calibration was developed using PyQt, Fig. 2. It has 4 tabs. The first 3 tabs are designed to run the main procedures for flow rate calibration including channel priming, flow rate calibration, and flow rate verification. The 4th tab is for selecting an individual channel to inject a solution for a user-defined amount of time for illuminating bubbles before setting up an imaging experiment. Calibration data and the resulting injection time (from a user defined volume to inject) for each channel will be saved as *.npy* files by the app. In this demonstration with a use case in our lab, the resulting injection times for each channel in the *.npy* file named *WaitTime.npy* can be transferred into a NIS-Element (Nikon software for imaging) Macro file and used in NIS-Element's ND acquisition with time-lapse imaging. Nikon NIS-Element macro codes are provided in the project's repository for running the 14-round sequential FISH imaging on pan alpha satellite in HeLa cell as a demonstration experiment with the fluidics system.

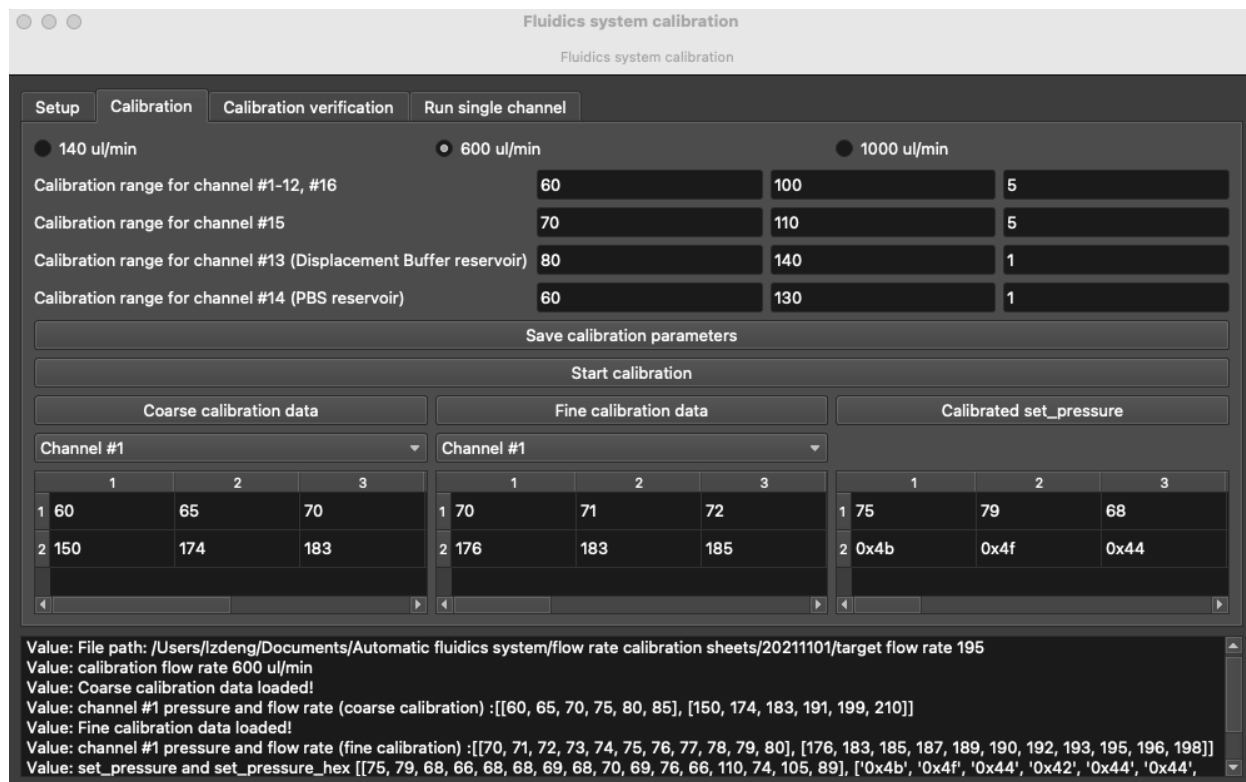


Fig. 2. The GUI for the automatic calibration of the fluidics system. Shown here is the calibration tab with calibration parameters configured for target flow rate 600 $\mu\text{L}/\text{min}$.

3. Design files summary

Design file name	File type	Open source license	Location of the file
bill_of_materials.xlsx	XLSX	GPL	Available with the article
fluidics_system_controller_PCB_design_files.zip	PCB files, KiCAD	GPL	https://doi.org/10.17632/tkm4w7wp3v.1 ; https://github.com/dzhaojie/Fluidics-system-for-FISH
Eppendorf_tube_adaptor_3D_print_files.zip	STL	GPL	https://doi.org/10.17632/tkm4w7wp3v.1 ; https://github.com/dzhaojie/Fluidics-system-for-FISH
laser_cut_acrylic_panel_organizer.ai	Illustrator file	GPL	https://doi.org/10.17632/tkm4w7wp3v.1 ; https://github.com/dzhaojie/Fluidics-system-for-FISH
controller_case_laser_cut.zip	3dm file	GPL	https://doi.org/10.17632/tkm4w7wp3v.1 ; https://github.com/dzhaojie/Fluidics-system-for-FISH
case_for_pressure_regulator_laser_cut.pdf	PDF	GPL	https://doi.org/10.17632/tkm4w7wp3v.1 ; https://github.com/dzhaojie/Fluidics-system-for-FISH
large_reservoir_holder.stl	STL	GPL	https://doi.org/10.17632/tkm4w7wp3v.1 ; https://github.com/dzhaojie/Fluidics-system-for-FISH

user_interface_app_for_flow_rate_calibration.zip	Python script	MIT	https://doi.org/10.17632/tkm4w7wp3v.1 ; https://github.com/dzhaojie/Fluidics-system-for-FISH
NIS-Element Macro codes.zip	.mac	MIT	https://doi.org/10.17632/tkm4w7wp3v.1 ; https://github.com/dzhaojie/Fluidics-system-for-FISH
Fluidics System Controller with ESP32	C++ code	MIT	https://doi.org/10.17632/tkm4w7wp3v.1 ; https://github.com/dzhaojie/Fluidics-system-for-FISH

bill_of_materials.xlsx: There are 8 sheets in this file. Except the sheets named ‘Tubings’ and ‘Remaining components’, each sheet lists components for a module and/or assembly described in the step-by-step building guide in the supplementary materials.

fluidics_system_controller_PCB_design_files.zip: KiCAD design files for the controller PCB

Eppendorf_tube_adaptor_3D_print_files.zip: STL files for 3D printing the Eppendorf tube adaptor and the slot panel that is designed for arranging and securing the adaptors

laser_cut_acrylic_panel_organizer.ai: Illustrator file for laser cutting the panels for assembling the structural frame and the Eppendorf tube adapter array

controller_case_laser_cut.3dm: Rhinoceros design file for laser cutting the controller case

case_for_pressure_regulator_laser_cut.pdf: pdf file for laser cutting the pressure regulator case

large_reservoir_holder.stl: STL file for 3D printing the large reservoir holders for securing large glass bottles for the washing buffer and displacement buffer used in the 14-round sequential FISH imaging demonstration experiment

user_interface_app_for_flow_rate_calibration.zip: Python scripts for the user interface app for automatic flow rate calibration

NIS-Element_Macro_codes.zip: Folder with NIS-Element Macro code for running the fluidics system and routines for the fluid exchange in the 14-round sequential FISH imaging demonstration experiment

Fluidics System Controller with ESP32: Folder with source code for the firmware of the controller PCB

4. Bill of materials summary

A separate bill of materials file named “bill_of_materials.xlsx” is included in the supplementary materials with multiple sheets. Each sheet lists parts for an individual module and/or assembly that makes up the fluidic system. The table below lists all the parts from that file. The cost for the component is listed in currency USD.

Designator	Component	Number	Cost per unit - currency	Total cost - currency	Source of materials	Material type
T1	Polyurethane Tubing for Air and Water, 5/32" ID, 1/4" OD, Clear Colors, 50 ft roll	5648K69	23.5	23.5	McMaster-Carr	Polymer
T2	Saint-Gobain™ Tygon™ ND 100-80 Tubing (500' roll,	14-171-284	325.5	325.5	Fisher Scientific	Polymer

	0.06" OD, 0.02" ID)					
T3	Polyurethane Tubing for Air and Water, 1/16" ID, 1/8" OD, Clear Colors	5648K67	6.5	6.5	McMaster- Carr	Polymer
T4	E-3603 Tygon PVC Tubing for Chemicals, 1/16" ID, 1/8" OD	5155T12	17.5	17.5	McMaster- Carr	Polymer
T5	E-3603 Tygon PVC Tubing for Chemicals 1/8" ID, 3/16" OD	5155T16	29.5	29.5	McMaster- Carr	Polymer
T6	Tubing, 50A Durometer, 0.058 inch ID x 0.077 inch OD (1.5 mm x 2 mm), 50 ft coil (15.24 m)	T2007	10.5	10.5	QOSINA	Polymer
P1	ESP32- DevKitC	ESP32- DevKitC	10	10	Espressif	Semiconductor
P2	PCA9698	PCA9698 DGG,518	4.53	13.59	NXP	Semiconductor
P3	UNL2803A	ULN2803 ADW	1.51	22.65	TI	Semiconductor
P4	TLV2374	296- 11967-1- ND	1.81	9.05	DigiKey	Semiconductor
P5	2.54mm Pitch, 0.64mm Width H-DAC 64 High Density Automotive Connectors, Dual Row, Female Harness Assembly, 16 Circuits, Polarization Option 1, Natural	538- 30700- 1167	2.02	30.3	Molex	Polymer
P6	2.54mm Pitch, H-DAC 64 High Density	538- 30700- 4160	2.49	37.35	Molex	Polymer

	Automotive Header, Dual Row, Vertical, 16 Circuits, Polarization Option 1, Natural, Tray					
P7	Cable Crimp	1393366-1	0.2	50	DigiKey	Metal
P8	Polarized Connectors - Housing (4-Pin)	PRT-08097	0.45	2.25	SparkFun	Polymer
P9	Polarized Connectors - Crimp Pins	PRT-08100	1.95	1.95	SparkFun	Polymer
P10	Polarized Connectors - Header (4 pin)	PRT-0823	0.45	0.9	SparkFun	Polymer
P11	DC Barrel Jack Adapter - Breadboard Compatible	PRT-10811	0.95	0.95	SparkFun	Polymer
P12	Wall Adapter Power Supply - 12VDC 600mA	TOL-09442	5.59	5.59	SparkFun	Other
P13	12 V to 5 V regulator	R-78E5.0-1.0	3.26	3.26	DigiKey	Semiconductor
P14	12 V to 24 V regulator	DSN6009	10.99	10.99	Amazon	Semiconductor
P15	Stackable Header - 3 Pin	PRT-13875	0.5	0.5	SparkFun	Polymer
P16	12 V to 9 V regulator	R-78E9.0-0.5	2.89	2.89	DigiKey	Semiconductor
P17	Pin header for ESP32 for	PRT-00115	1.5	6	SparkFun	Polymer
P18	0.1 uF capacitor	1276-1007-1-ND	0.1	2	digiKey	Semiconductor
P19	6.8 uF capacitor	478-8447-1-ND	0.79	3.95	digiKey	Semiconductor
P20	10 uF capacitor	445-14484-1-ND	0.38	3.8	digiKey	Semiconductor
P21	1.6 K resistor	P20615C T-ND	0.36	3.6	digiKey	Semiconductor
P22	1.8 K resistor	P20621C T-ND	0.36	3.6	digiKey	Semiconductor
P23	3.3 K resistor	P20651C T-ND	0.36	3.6	digiKey	Semiconductor
P24	Printed PCB board	N/A	121.33	121.33	OSHPARK	Semiconductor

S1	20mm X 20mm T- Slotted Profile - Four Open T-Slots - 30 inches	20-2020	6.75	27	80/20, LLC	Metal
S2	20mm X 20mm T- Slotted Profile - Four Open T-Slots - 12 inches	20-2020	3.87	46.44	80/20, LLC	Metal
S3	20 Series 2 Hole - Inside Corner Bracket	20-4119	2.85	68.4	80/20, LLC	Metal
S4	5.30mm ID Washer	Nov-40	0.11	5.28	80/20, LLC	Metal
S5	M5 Slide-in Economy T- Nut Block	14122	0.21	16.8	80/20, LLC	Metal
S6	M5 x 10.00mm Button Head Socket Cap Screw	13-5310	0.24	11.52	80/20, LLC	Metal
S7	45mm X 45mm T- Slotted Profile - Four Open T-Slots - 22 inches	45-4545- Black-FB	20.12	40.24	80/20, LLC	Metal
S8	45 Series 2 Hole - Gusseted Inside Corner Bracket	45-4332- Black	5.26	21.04	80/20, LLC	Metal
S9	Bolt Assembly: M8 x 18.00mm Black BHSCS with Standard Drop-In T-Nut - Bright Zinc	75-3619	1.15	4.6	80/20, LLC	Metal
S10	8.51mm ID Washer	11-6042	0.13	0.52	80/20, LLC	Metal
S11	Post- Assembly T- Slot Nuts, M5	26016-01	10.49	20.98	Inventables	Metal
S12	Laser cut acrylic panel (3/16" thick), tubing organization	N/A	9.4	9.4	Custom laser cut	-Other

S13	Laser cut acrylic panel (3/16" thick), tubing organization	N/A	9.4	9.4	Custom laser cut	-Other
S14	Laser cut acrylic panel (3/16" thick), tubing organization	N/A	9.4	9.4	Custom laser cut	-Other
S15	Laser cut acrylic panel (3/16" thick), tubing organization	N/A	9.4	9.4	Custom laser cut	-Other
O1	Valco manifolds	Z16M1PK	300	300	Valco Instruments Co. Inc.	Polymer
O2	Super-Corrosion-Resistant 316 Stainless Steel Socket Head Screw, M6 x 1 mm Thread, 30 mm Long	92290A33 2	17.5	17.5	McMaster-Carr	Metal
O3	18-8 Stainless Steel Hex Nut, M6 x 1 mm Thread	91828A25 1	14.73	14.73	McMaster-Carr	Metal
O4	Duckbill Check Valve; Yellow Inlet, Clear Outlet	80089	1.28	25.6	QOSINA	Polymer
O5	One-way luer check valve, SAN with silicone diaphragm, female-male	EW-30505-92	9.7	9.7	Cole-Parmer	Polymer
O6	Idex P-628 Threaded Luer Adapter, Natural ETFE, 0.040" Bore, Female Luer x Female 1/4-28 Flat Bottom	UX-02014-03	4.49	22.45	Cole-Parmer	Polymer
E1	3D printed adapter body	N/A	0.24	7.68	Custom 3D print	Polymer
E2	Tapered Heat-Set Inserts for Plastic	93365A26 0	13.12	26.24	McMaster-Carr	Metal

	1/4"- 28 Thread Siz e, 1/2" Installe d Length, Bra ss					
E3	Oil- Resistant Har d Buna-N O- Ring, 2 mm Wide, 6 mm ID	1247N17 3	3.71	3.71	McMaster- Carr	Other
E4	Flangeless Male Nut Delrin®, 1/4- 28 Flat- Bottom, for 1/8" OD - White	P-303	1.39	55.6	IDEX Health & Science	Polymer
E5	Flangeless Ferrule Tefzel™ (ETF E) 1/4-28 Flat-Bottom, for 1/8" OD	P-300	1.39	55.6	IDEX Health & Science	Polymer
E6	Flangeless Male Nut Delrin®, 1/4- 28 Flat- Bottom, 1/16" OD	P-202X	12.1	48.4	IDEX Health & Science	Polymer
E7	Flangeless Ferrule Tefzel™ (ETF E), 1/4-28 Flat-Bottom, for 1/16" OD	P-200	1.39	55.6	IDEX Health & Science	Polymer
E8	3D printed slot panel for Eppendorf tube adaptor	N/A	0.75	0.75	Custom 3D print	Polymer
E9	Laser cut bottom panel (3/16" thick), Sample loading module assembly	N/A	9.4	9.4	Custom laser cut	Polymer
E10	Laser cut top panel (3/16" thick), Sample loading module assembly	N/A	9.4	9.4	Custom laser cut	Polymer
E11	18-8 Stainless Steel Socket	91292A02 6	4.77	4.77	McMaster- Carr	Metal

	Head Screw M3 x 0.5 mm Thread, 50 mm Long					
E12	Zinc-Plated Steel Hex Nut Low-Strength, M3 x 0.5 mm Thread	90591A12 1	1.9	1.9	McMaster- Carr	Metal
E13	Low-Strength Zinc-Plated Steel Threaded Rod, M5 x 0.8 mm Thread, 300 mm long	94595A21 7	5.61	11.22	McMaster- Carr	Metal
E14	Zinc- Plated Steel High Hex Nut, Class 6, M5 x 0.8 mm Thread	90725A03 0	9.55	9.55	McMaster- Carr	Metal
E15	316 Stainless Ste el Washer, for M5 Screw Size, 5.3 mm ID, 10 mm OD	90965A16 0	4.77	4.77	McMaster- Carr	Metal
SV1	Pneumadyne 3-way normally open Solenoid Valves	S10MM- 30-12-2	30.01	600.2	Pneumadyne	Non-specific
SV2	10-Station Solenoid Manifolds	MSV10- 10	36.4	72.8	Pneumadyne	Metal
SV3	1/16 Tube Id Barb Straight Connectors (10-32 UNF)	EB10	42.5	42.5	Pneumadyne	Metal
SV4	Push-to- Connect Tube Fitting for Air & Water, Straight Adapter, 1/4" Tube OD x 10-32 UNF Male	7880T122	2.89	5.78	McMaster- Carr	Metal
SV5	Black-Oxide Alloy Steel Socket Head Screw M3 x 0.5 mm	91290A57 2	10	10	McMaster- Carr	Metal

	Thread, 15 mm Long					
SV6	Post-Assembly T-Slot Nuts, M3 (3mm) × 0.5	26016-02	10.49	10.49	Inventables	Metal
C1	BC-222N - BOTTLE CAP, GL45 2-ported 1/4-1/4-28, PTFE	BC-222N	25	50	Chrom Tech	Other
C2	BT45-1B - BOTTLE GL45 1 Liter, Clear Glass Press Resist	BT45-1B	25	50	Chrom Tech	Other
C3	μ-Slide VI 0.5 Glass Bottom	80607	16	16	ibidi	Other
C4	Elbow Luer Connector Male	10802	3	6	ibidi	Polymer
C5	Polycarbonate, Straight, Male Luer Lock to Hosebarb Adapter, 1/8" ID	EW-45504-04	16.6	16.6	Cole-Parmer	Polymer
C6	Male to Male Luer Lock Connector	12090	0.14	0.14	QOSINA	Polymer
C7	Check Valve, Female Luer Lock Inlet, Male Luer Lock Outlet	80129	0.88	0.88	QOSINA	Polymer
R1	Microfluidic thermal flow sensor	LVF-MFS-D-4	1,872	1872	DARWIN microfluidics	Non-specific
R2	Campbell Hausfeld Air Cleaner, Air Dryer for Air Tools	PA20850 3AV	80	80	Amazon	Non-specific
R3	MPV Pressure Regulator	MPV1PA NKKZP15 PSGAAL	541	541	ProportionAir	Non-specific
R4	Push-to-Connect Tube Fitting for Air & Water, Straight Adapter, 1/4" Tube OD x 1/4 NPT Male	7880T125	2.24	4.48	McMaster-Carr	Metal

R5	Push-to-Connect Tube Fitting for Air & Water, Straight Adapter, 1/4" Tube OD x 1/8 NPT Male	7880T124	2.24	6.72	McMaster-Carr	Metal
R6	2-Station, 3/8 NPT (F) Input, Aluminum Manifold	M20-250-2	14.47	14.47	pneumadyne	Metal
R7	Push-to-Connect Tube Fitting for Air & Water, Straight Adapter, 1/4" Tube OD x 3/8 NPT Male	7880T126	2.72	5.44	McMaster-Carr	Metal
R8	High-Pressure Brass Pipe Fitting, Solid Plug with External Hex Drive, 3/8 NPT	50785K336	2.96	2.96	McMaster Carr	Metal
R9	Bubble Trap for Microfluidics Kit	LVF-3525	128	128	DARWIN microfluidics	Non-specific

5. Build instructions

A step-by-step guide for building the fluidics system is provided in the supplementary materials. There are 7 sections in the guide each describing an individual module and/or assembly with the last section about connecting everything together.

6. Operation instructions

A calibration and operation guide is provided in the supplementary materials. With the 14-round fluor oligo exchange to image pan-alpha satellite in HeLa cell as example, the instruction describes step-by-step the calibration and operation procedure for setting up the fluidics system for automatic liquid handling for the imaging experiment.

7. Validation and characterization

7.1 Flow rate control

A robust flow rate control is important for controlling the injection volume. The flow rate is linearly proportional to the amount of pressure that is applied to the reservoir. A calibration routine is integrated into the user interface. This routine can complete the automatic flow rate calibration with the 1.5 ml PBS buffer that is loaded in the 2 mL Eppendorf tube. This helps to minimize the sample loading effort for calibration. By default, 3 target flow rates, 140 $\mu\text{L}/\text{min}$, 630 $\mu\text{L}/\text{min}$ (denoted by 600 $\mu\text{L}/\text{min}$ in the

calibration tab in the user interface), and 995 $\mu\text{L}/\text{min}$ (denoted by 1000 $\mu\text{L}/\text{min}$ in the calibration tab in the user interface) can be selected from the user interface with tested calibration parameters. The flow rate calibration routine that can calibrate all 16 channels without any human interaction takes about 40 mins. Table 1, Table 2, and Table 3 shows the measured flow rate for all 16 channels for the 3 target flow rates respectively. The average accuracy of the 16 channels is $\pm 5\%$ of the target flow rate.

Table 1. Flow rate calibration result of target flow rate = 140 $\mu\text{L}/\text{min}$. Mean and standard deviation (SD) are based on 3 measurements.

Channel no.	Target flow rate = 140 $\mu\text{L}/\text{min}$			
	Measured flow rate ($\mu\text{L}/\text{min}$)		Percentage error	
	Mean	SD	Mean	SD
1	139.93	2.59	1.38	0.76
2	141.73	9.07	4.57	3.60
3	142.76	7.80	4.93	0.63
4	144.58	7.56	4.67	3.54
5	140.93	6.10	3.11	2.26
6	143.16	2.75	2.25	1.96
7	142.21	9.93	5.55	2.78
8	145.81	5.41	4.15	3.86
9	141.69	6.10	3.66	1.06
10	145.47	10.06	4.32	6.82
11	144.26	8.48	5.49	2.31
12	141.01	3.48	2.12	0.46
13	153.93	10.38	9.95	7.41
14	146.61	2.14	4.72	1.53
15	150.27	0.75	7.34	0.53
16	146.29	6.44	4.50	4.60

Table 2. Flow rate calibration result of target flow rate = 630 $\mu\text{L}/\text{min}$. Mean and standard deviation (SD) are based on 3 measurements.

Channel no.	Target flow rate = 630 $\mu\text{L}/\text{min}$			
	Measured flow rate ($\mu\text{L}/\text{min}$)		Percentage error	
	Mean	SD	Mean	SD
1	635.30	14.91	1.94	1.00
2	628.32	6.29	0.83	0.28
3	634.13	6.13	0.83	0.74
4	631.81	14.91	1.76	1.04
5	642.28	13.85	1.95	2.20
6	636.46	5.61	1.03	0.89
7	635.88	16.50	1.67	2.00
8	639.95	15.84	2.31	1.43
9	641.70	16.12	2.59	1.29
10	636.46	7.05	1.03	1.12
11	647.51	7.61	2.78	1.21
12	634.13	21.11	2.31	1.98
13	629.48	5.33	0.64	0.33
14	639.95	8.78	1.58	1.39
15	636.46	7.05	1.20	0.81
16	640.53	10.62	1.85	1.38

Table 3. Flow rate calibration result of target flow rate = 995 $\mu\text{L}/\text{min}$. Mean and standard deviation (SD) are based on 3 measurements.

Channel no.	Target flow rate = 995 $\mu\text{L}/\text{min}$			
	Measured flow rate ($\mu\text{L}/\text{min}$)		Percentage error	
	Mean	SD	Mean	SD
1	949.47	19.00	4.58	1.91
2	973.90	3.63	2.12	0.36
3	978.09	4.19	1.70	0.42
4	998.34	12.27	1.05	0.21
5	1000.43	19.00	1.54	0.74
6	985.07	10.75	1.13	0.87
7	987.17	15.86	1.48	0.44
8	979.49	1.21	1.56	0.12
9	966.22	7.36	2.89	0.74
10	990.66	15.81	1.27	0.63
11	978.09	2.09	1.70	0.21
12	982.98	18.77	1.21	1.89
13	976.69	3.20	1.84	0.32
14	970.41	7.93	2.47	0.80
15	990.66	9.13	0.57	0.80
16	989.96	29.64	2.46	0.42

7.2 Minimum injection volume

The fluidic system is designed and built to minimize dead volume (the volume of reagent that used to fill up one individual channel before injecting into the imaging chamber) to reduce reagent cost, especially those of fluorescence oligos. The total dead volume measured by filling one individual channel with DI water is about 200 μL (volume of ~ 1.5 ft of 0.02" ID tubing (~ 90 μL) + volume of the one-way check valve (~ 20 μL) + dead volume of the 16-1 manifold (~ 1.4 μL) + dead volume of in-line bubble remover (~ 90 μL)). However, for a channel that is primed with a priming reagent (PBS or DI water), it would be required to inject volume more than this amount to ensure the concentration of the injected reagent when reaching the imaging chamber is maximum (equal to the concentration of the reagent in the Eppendorf tube reservoir). The minimum injection volume (when a channel is primed with PBS) for the reagent concentration to reach maximum in the imaging chamber is empirically determined by an experiment. During the experiment, images of the imaging chamber were recorded every 3 seconds in real-time for each channel from when the reagent (a blue dye is used here, ELVEFLOW Microfluidic Dyes Channels Visualization Kit, SKU: LVF-KXX-06) is injected and the imaging lasted for 75 s for each channel. Between switching channels, 2 mL 1XPBS was injected to wash out the dye from the previous channel and the fluorescence intensity of image of the imaging chamber is verified to decrease to minimum after the washing. The resulting averaged fluorescence intensities change over time for each channel is shown in the plot in Fig. 3. Channel # 1-12, # 15, and # 16 is shown here. Channel # 14 was used for injecting 1X PBS for washing during the experiment. Channel # 13 is not used for this experiment since it is designated for injecting a displacement buffer (for FISH) in the actual sequential FISH experiment. Also, the flow rate is recorded in real-time for estimating the minimum injection volume. The minimum injection volume is estimated as the volume that has been injected when the fluorescence intensity in the imaging chamber first reaches 98% of that in the Eppendorf tube reservoir. Table 4 shows the resulting minimum injection volume for each channel. For all the channels, the injection volume calculated based on this experiment shows to be < 800 μL . Therefore, 800 μL is used as the default minimum injection volume.

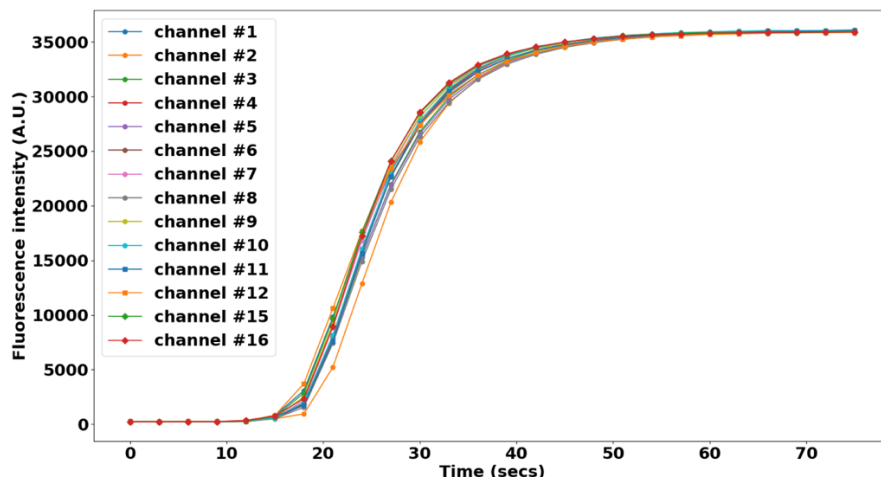


Fig. 3. Fluorescence intensity time course during dye injection for 14 channels: channel # 1-12, # 15 and 16. Each data point is the average fluorescence intensity of an image. The images were taken every 3 secs from the onset of the dye injection from one channel till the 75 secs end time. Flow rate is 1 mL/min.

Table 4. Minimum injection volume for fluorescence intensity reaches plateau in the imaging chamber. This is calculated from Fig. 3. The minimum injection volume is determined by the time at which the fluorescence intensity reaches 98% of the maximum fluorescence intensity in the plot.

Channel no.	Injection time (s)	Minimum injection volume (μL)
1	42	786
2	42	770
3	42	793
4	39	757
5	42	777
6	42	774
7	39	722
8	42	787
9	39	703
10	39	732
11	42	765
12	42	760
15	39	748
16	39	710

7.3 Minimal cross-contamination validation

An experiment was designed and carried out to evaluate the degree of cross-contamination between channels. Reservoirs for channels # 1-12 and 15, 16 were loaded with fluorescent oligos following this order and then repeat it: 488-oligo, 565-oligo, 647-oligo. Reservoirs for channel #13 were loaded with 1X PBS as a washing buffer. And all the channels were primed with PBS. Images were taken in three fluorescence channels (488, 565, 647) after injecting 800 μL (the minimum injection volume from 7.2) fluorescence oligos from one fluidics channel. 2 mL of 1X PBS was injected afterwards and images were then taken again (in three fluorescence channels). These were repeated from the first fluidics channel until the last fluidics channel. Once the reagents are loaded the experiment routine was run automatically with injection commands issued and images taken by NIS-Element. The average fluorescence intensities in the three fluorescence channels are shown in Fig. 4. The order of which fluorescence channel has maximum intensity value follows the order of the fluorescent oligos being injected. Moreover, the fluorescence channels that are not associated with the intended injected fluorescent oligos have very low intensity values. The fluorescence intensity value is also low when 1X PBS was injected to wash the oligo

away from the imaging chamber. The fluorescence intensity is very consistent across channels when the same fluorescent oligos is injected. These results show that sequential injection with the fluidics system combined with imaging can be successfully carried out without significant cross-contamination between channels and the concentration of reagent injected from each channel remains consistent.

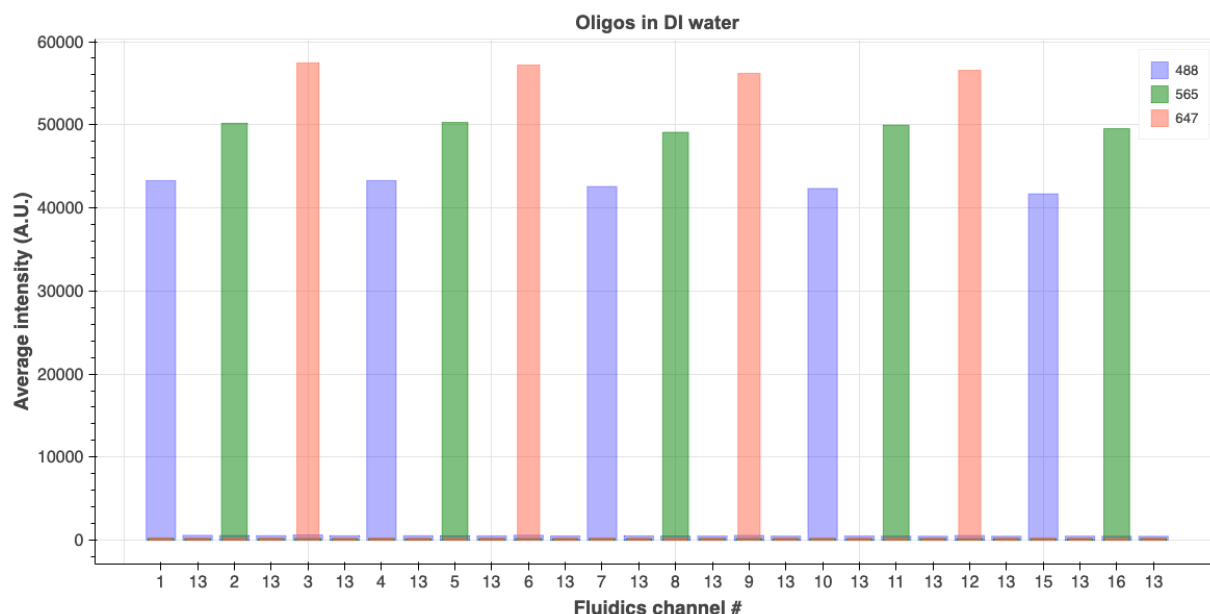


Fig. 4. Average fluorescence intensity of images taken in fluorescence imaging channels: 488 nm, 565 nm, and 647 nm. Fluorescence oligos were loaded into the Eppendorf tube reservoirs in this order: 488-oligo for channel 1, 565-oligo for channel 2, 647-oligo for channel 3 and this order was repeated for channels # 4-12 and # 15 and # 16. Images were taken after 800 μ L fluorescence oligos reagent from one channel was injected. 2 mL 1X PBS was injected as a washing step to wash out the oligos from the previous injection before injecting fluor oligos from the next channel. Images were also taken after the 2 mL 1X PBS injection finished for that round.

7.4 Automating a sequential FISH-based imaging experiment

To demonstrate the fluidics system's capability of performing oligo probe exchange for sequential FISH-based imaging, an experiment was carried out using DNA-SABER FISH to target the alpha satellite repeat in HeLa cells with three different fluorescent readout oligos. The imaging chamber (1 channel of an ibidi 6-channel slide) was first seeded with HeLa cells and primary FISH probes were hybridized before the imaging chamber was connected to the fluidics system. Each of the primary probes has a SABER [19] concatemer sequence (the 'p27' concatemer sequence) that can be targeted by SABER fluorescent oligos as readout probes. Three different SABER fluorescent oligos were loaded into the Eppendorf tubes for fluidics channels # 1-12, channels # 15 and 16 in the following order and then repeat: p27-488, p27-565, p27-647. Reservoirs for channels # 13 and 14 were loaded with a displacement buffer and 1X PBS separately. Fluorescent oligos were injected sequentially and images were taken once the oligos from the current fluidics channel were incubated in the imaging chamber for 1 h (hybridization step) and after the oligos were stripped away by injecting the displacement buffer (washing step). The displacement buffer consisted of 0.4X PBS + 0.04% (vol/vol) Tween-20 + 60% (vol/vol) formamide. The fluorescent oligos exchange and imaging routines were controlled by NIS-Element communicating with the fluidics system's controller by serial commands. No human intervention was needed once the experiment started to run. A detailed protocol for the fluorescence oligo exchange is included in the supplementary materials. The fluorescence images for the first three rounds of hybridization are shown in Fig. 5 (A). The alpha satellite pattern was illustrated by the corresponding fluorescence oligos. Zoom-in images of one cell from Fig. 5 (A) are shown in Fig. 5 (B). The average pixel intensity was quantified by averaging the fluorescence intensity of pixels belonging to the alpha satellite puncta. This is shown in the plot in Fig. 5 (C). The plot shows that the intensity has the highest value in the imaging channel that is associated with the intended injected fluorescent oligos and the intensity is very low in the other two imaging channels. Also, the

intensity from images taken after introducing the displacement buffer is low (images taken after the washing step in each cycle). The decrease of intensity in the plot over cycles is likely due to the instability of the fluorescent oligos in the PBS buffer. Nevertheless, the result demonstrates that the fluidics system is robust in handling complicated fluidics exchange routines for sequential FISH-based imaging.

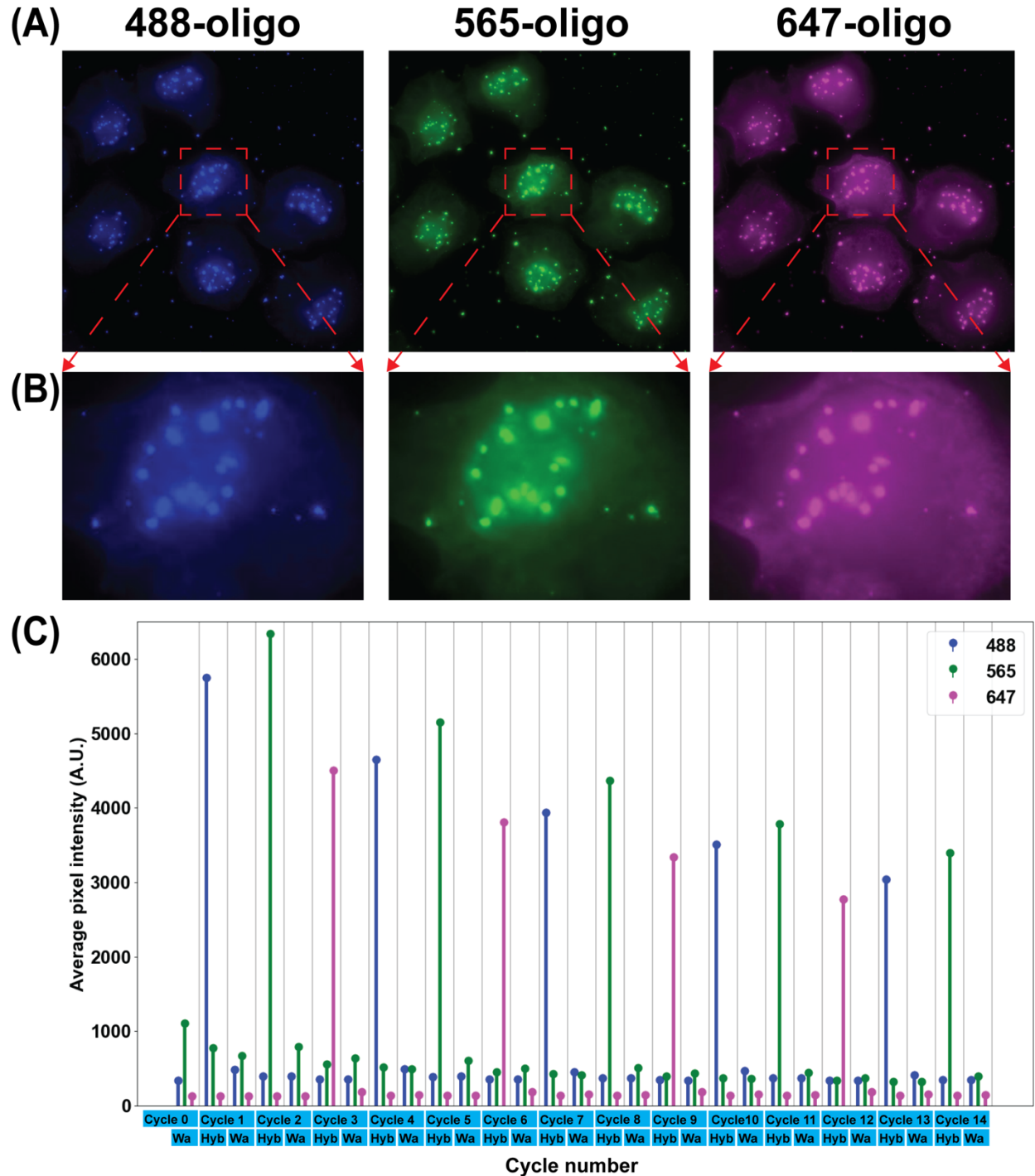


Fig. 5. Result of the sequential FISH-based imaging targeting pan-alpha in HeLa cell. (A) Images taken after injecting fluorescence oligos from fluidics channel # 1, 2, and 3 (after the hybridization step in Cycle 1, 2 and 3). (B) Zoom-in images of one cell from (A). (C) The average pixel intensity of pan-alpha puncta in images taken in fluorescence imaging channels 488 nm, 565 nm, and 647 nm in each Cycle. Cycle 1 to 12 inject fluorescence oligos from fluidics channels #1 to 12, Cycle 13 and 14 inject fluorescence oligos

from fluidics channels # 15 and 16. Each cycle includes a hybridization step (indicated as Hyb in the x axis) followed by a washing step (indicated as Wa in the x axis) except Cycle 0. Cycle 0 only has a washing step. Images were taken after the hybridization step as well as after the washing step in each cycle.

CRedit author statement

Zhaojie Deng: Conceptualization, Methodology, Software, Writing- Original draft preparation. Brian J. Beliveau: Conceptualization, Methodology, Writing- Reviewing and Editing.

Acknowledgments

The authors thank Dan Fong (Nikon) for technical support with the Nikon microscope and NIS-Element software, Sahar Attar (Beliveau Lab) for help with primary FISH, Eva Kristine Nichols, Yuzhen Liu, Chris Hsu (Beliveau Lab) for providing ibidi slides with seeded cells, and all the Beliveau Lab members for their helpful feedback on the draft manuscript and figures. We also thank the Maker Space in the University of Washington for providing resources for PCB debugging, laser cutting and 3D printing. This work was supported by a Damon Runyon Dale F. Frey Breakthrough Award (to B.J.B.), the National Institutes of Health (under grant no. 1R35GM137916 to B.J.B.), and a Brotman Baty Catalytic Collaborations Award (to B.J.B.).

References:

- [1]. E. Lubeck, L. Cai. Single-cell systems biology by super-resolution imaging and combinatorial labeling. *Nat Methods* 9, (2012) 743–748. <https://doi.org/10.1038/nmeth.2069>
- [2]. M. Levesque, A. Raj. Single-chromosome transcriptional profiling reveals chromosomal gene expression regulation. *Nat Methods* 10, (2013) 246–248. <https://doi.org/10.1038/nmeth.2372>
- [3]. S. Wang *et al.* Spatial organization of chromatin domains and compartments in single chromosomes. *Science* 353, (2016) 598–602. <https://doi.org/10.1126/science.aaf8084>
- [4]. B. Bintu *et al.* Super-resolution chromatin tracing reveals domains and cooperative interactions in single cells. *Science* 362, (2018). <http://doi.org/10.1126/science.aau1783>
- [5]. A. M. Gardozo Gizzi *et al.* Microscopy-based chromosome conformation capture enables simultaneous visualization of genome organization and transcription in intact organisms. *Molecular Cell* 74, (2019) 212–222. <https://doi.org/10.1016/j.molcel.2019.01.011>
- [6]. L. J. Mateo *et al.* Visualizing DNA folding and RNA in embryos at single-cell resolution. *Nature* 568, (2019) 49–54. <https://doi.org/10.1038/s41586-019-1035-4>
- [7]. K. K. Chen *et al.* Spatially resolved, highly multiplexed RNA profiling in single cells. *Science* 348, (2015). <http://doi.org/10.1126/science.aaa6090>
- [8]. S. Shah *et al.* Dynamics and Spatial Genomics of the Nascent Transcriptome by Intron seqFISH. *Cell* 174, (2018) 363–376. <https://doi.org/10.1016/j.cell.2018.05.035>
- [9]. J-H. Su *et al.* Genome-Scale Imaging of the 3D Organization and Transcriptional Activity of Chromatin. *Cell* 182, (2020) 1641–1659. <https://doi.org/10.1016/j.cell.2020.07.032>

- [10]. Y. Takei *et al.* Integrated spatial genomics reveals global architecture of single nuclei. *Nature* 590, (2021) 344–350. <https://doi.org/10.1038/s41586-020-03126-2>
- [11]. Sequential fluid injection pack – ElveFlow. Available at: <https://www.elveflow.com/microfluidic-applications/setup-microfluidic-flow-control/peristaltic-pump-compared-to-pressure-driven-flow-control/>. (Accessed: 28, January 2022)
- [12]. Sequential perfusion system – Aria | FLUIGENT. Available at <https://www.fluigent.com/research/instruments/aria/>. (Accessed: 28, January 2022)
- [13]. Microfluidics Unit – BRUKER. Available at: <https://www.bruker.com/en/products-and-solutions/fluorescence-microscopy/super-resolution-microscopes/microfluidics-unit.html>. (Accessed: 28, January 2022)
- [14]. P. Rodriguez-Mateos, N. Filipe Azevedo, C. Almeida, N. Pamme, FISH and chips: a review of microfluidic platforms for FISH analysis. *Med Microbiol Immunol* 209, (2020) 373–391. <https://doi.org/10.1007/s00430-019-00654-1>
- [15]. J.R. Moffitt, X. Zhuang, RNA Imaging with Multiplexed Error-Robust Fluorescence In Situ Hybridization (MERFISH), in: G. Filonov (Ed.), *Visualizing RNA Dynamics in the Cell*, *Methods in Enzymology*, 572, (2016) 1-49. <https://doi.org/10.1016/bs.mie.2016.03.020>
- [16]. P. Almada *et al.* Automating multimodal microscopy with NanoJ-Fluidics. *Nat Commun* 10, (2019) Article 1223 <https://doi.org/10.1038/s41467-019-09231-9>
- [17]. Peristaltic pumps vs. pressure driven flow control – ElveFlow. Available at: <https://www.elveflow.com/microfluidic-applications/setup-microfluidic-flow-control/peristaltic-pump-compared-to-pressure-driven-flow-control/>. (Accessed: 28, January 2022)
- [18]. C. Watson, S. Senyo, All-in-one automated microfluidics control system. *HardwareX* 5, (2019) Article e00063 <https://doi.org/10.1016/j.ohx.2019.e00063>
- [19]. J.Y. Kishi *et al.* SABER amplifies FISH: enhanced multiplexed imaging of RNA and DNA in cells and tissues. *Nat Methods* 16, (2019) 533–544. <https://doi.org/10.1038/s41592-019-0404-0>